Influence of shear rate on the optical properties of human blood in the spectral range 250 to 1100 nm

Moritz Friebel
Jürgen Helfmann
Laser-und Medizin-Technologie GmbH, Berlin
Fabeckstrasse 60-62
14195 Berlin, Germany

Gerhard Müller
Martina Meinke
Charité - Universitätsmedizin Berlin
Campus Benjamin Franklin
Institut für Medizinische Physik und Lasermedizin
Fabeckstrasse 60-62
14195 Berlin, Germany
E-mail: martina.meinke@charite.de

Abstract. The intrinsic optical parameters—absorption coefficient μ_a, scattering coefficient μ_s, anisotropy factor g, and effective scattering coefficient μ_s'—are determined for human red blood cells of hematocrit 42.1% dependent on the shear rate in the wavelength range 250 to 1100 nm. Integrating sphere measurements of light transmittance and reflectance in combination with inverse Monte-Carlo simulation are carried out for different wall shear rates between 0 and 1000 s^{-1}. Randomly oriented cells show maximal μ_a, μ_s, and μ_s' values. Cell alignment and elongation, as well as the Fahraeus effect at increasing shear rates, lead to an asymptotical decrease of these values. The anisotropy factor shows this behavior only below 600 nm, dependent on absorption; above 600 nm, g is almost independent of shear rate. The decrease of μ_s' is inversely correlated with the hemoglobin absorption. Compared to randomly oriented cells, aggregation reduces all parameters by a different degree, depending on the hemoglobin absorption. It is possible to evaluate the influence of collective scattering phenomena, the absorption within the cell, and the cell shape.
[DOI: 10.1117/1.2799154]

Keywords: flow; shear rate; absorption coefficient; scattering coefficient; anisotropy factor; Monte Carlo simulation.

Paper 06381R received Dec. 22, 2006; revised manuscript received May 16, 2007; accepted for publication Jun. 1, 2007; published online Oct. 19, 2007.

1 Introduction

The development of spectroscopic methods for blood analysis requires knowledge of the light-scattering and absorption properties of human blood. It is also important for many diagnostic and therapeutic applications in laser medicine, hematology, and medical routine diagnosis.

According to the radiation transport theory, the optical properties of blood can be described by the intrinsic optical parameters: absorption coefficient μ_a, scattering coefficient μ_s, and anisotropy factor g, together with an appropriate phase function. Various approaches have been taken to determine the optical properties of blood.[1–10] Due to the high optical density of blood, especially at physiological concentrations, it has not been possible in most cases to determine the parameters μ_s and g separately. Only the effective scattering coefficient $\mu_s' = \mu_s\ (1-g)$ could be determined for single wavelengths or small spectral ranges where the absorption of hemoglobin is low. Using the double integrating sphere technique combined with an inverse Monte Carlo simulation (iMCS),[1,4–6] all three optical parameters of diluted, as well as undiluted, flowing blood could be determined independently in a spectral range of 250 to 1100 nm, including the spectral areas of high hemoglobin absorption. It is known that the optical behavior of blood depends on various physiological parameters such as oxygen saturation, pH, aggregation, and hematocrit.[11–15] One important parameter is the flow-induced shear force that can cause characteristic changes in cell morphology and organization of red blood cells.[3,16–24] The position-dependent shear force $\tau(x)$ can be described by the shear rate γ, which is defined as the velocity gradient in the direction normal to the flow and independent of the blood viscosity η.

$$\tau(x) = \gamma \cdot \eta = -\frac{dv}{dx} \cdot \eta, \tag{1}$$

where $v(x)$ is the position-dependent flow velocity.

In blood vessels under conditions of constant laminar flow, there is a radially dependent shear rate with a minimum at the center and a maximum at the wall of the vessel.[25] Flow-dependent changes in the optical properties have to be considered for numerous applications, such as blood oxymetry, determination of the Hct in cardiopulmonary systems, laser Doppler blood flowmetry, and diagnostic measurements of the erythrocyte aggregation/disaggregation behavior.[26–30]

The characteristic changes in cell morphology and organization of red blood cells (RBCs) can be linked to various ranges of shear rate.[23,24] At shear rates below 60 s^{-1} or at flow stop, RBCs show aggregation-forming rouleaux-shaped ag-

Address all correspondence to Martina Meinke, Institut für Medizinische Physik und Lasermedizin, Charité — Universitätsmedizin Berlin, Campus Benjamin Franklin, Fabeckstrasse 60-62-Berlin, Berlin 14195 Germany; Tel: 49–30–844 54158; Fax: 49–30–844 51289; E-mail: martina.meinke@charite.de

1083-3668/2007/12(5)/054005/8/$25.00 © 2007 SPIE

gregates, which disintegrate at higher shear rates. This aggregation is derived from plasma proteins. Washed RBCs form no aggregates and are randomly oriented at flow stop. RBCs in plasma show random orientation at shear rates between 100 to 200 s^{-1} when the aggregates are disintegrated. At shear rates exceeding 400 s^{-1}, RBCs are aligned, and finally, in the range above 1000 s^{-1}, they are deformed into ellipsoid with the long axis running parallel to the flow.[18,19]

In vessels of diameters below 300 μm, the RBCs tend to move near the center of the tube (transverse migration). This leads to a radial RBC concentration profile with a thin cell-free plasma layer close to the wall of the tube. Due to the velocity profile, a difference occurs between the mean velocities of RBCs and the suspending fluid, leading to a dynamic hematocrit Hct_D within the tube, which is lower than the static hematocrit Hct_S (Fahraeus effect).[25,31]

Gaehtgens, Albrechts, and Kreutz[32] found that the Fahraeus effect decreases with decreasing flow. In experiments using flow-through cuvettes, the effects of orientation, elongation, and transversal migration occur simultaneously. To exclude the influence of cell deformation in experiments, the RBCs can be fixed with glutaraldehyde, and substituting the blood plasma for saline solution can prevent cell aggregation.

The aim of the present study is to investigate the influence of shear rate on the optical properties of human blood at physiological Hct in the wavelength range 250 to 1100 nm. To do this, the optical parameters μ_a, μ_s, and g were determined for human RBCs dependent on the shear rate for six different values from 0 to 1000 s^{-1}. To facilitate comparison with data from the literature, μ_s' was also calculated. In the main investigations, native RBCs were suspended in saline solution to avoid aggregation. Cell aggregation at flow stop was investigated in additional experiments where the RBCs were suspended in plasma. Fixed cells were used to investigate the influence of cell elongation, and the influence of the Hct was investigated in selected experiments using diluted RBC suspensions of Hct 8.6%.

All shear rates given in this work are the wall shear rates at the cuvette window. Given a cuvette with a rectangular cross section (width $b \gg$ height d), the shear rate can be estimated for Newtonian fluids according to Eq. (2),[20]

$$\gamma_w = 6\frac{v_m}{d}, \tag{2}$$

where v_m is the mean flow velocity and d is the cuvette thickness.

The fact that blood is a non-Newtonian fluid and therefore exhibits higher wall shear rates has to be considered when comparing absolute values.[33] In the present experiments, the cuvette thickness is constant and therefore the mean flow velocity can be recalculated and used as a variable parameter instead of the shear rate. The wall shear rate was calculated to compare the data in this study with data from the literature where the same formula was used.[20]

The mean velocity v_m can be easily determined from the volume flow $\dot{V} = dV/dt$ according to $v_m = \dot{V}/bd$.

2 Materials and Methods

2.1 *Blood Preparation*

To measure native RBCs in saline solution, fresh human erythrocytes from healthy blood donors were centrifuged three times (1000 g) and washed with isotonic phosphate buffer (300 mosmol/L, pH 7.4) to remove the blood plasma and free hemoglobin. This procedure does not influence the biological function of the RBCs, but inhibits the formation of aggregates. The blood concentration was varied by diluting the sample with buffer. Two different hematocrit values, 8.6 and 42.1%, were investigated. The suspensions with Hct 42.1% of native intact RBCs are referred to as "RBC in NaCl" in the diagrams shown in the chapter results. To investigate the influence of flow-induced changes on the cell shape, the RBCs of one blood sample were fixed by treatment with glutaraldehyde (0.15%). The treatment of the cell membrane with glutaraldehyde fixed the red blood cell in the normal biconcave shape. This suspension of non-native RBCs is called "RBC fixed." To study the aggregation phenomena, RBCs of another sample were suspended in human plasma by replacing the supernatant with cell-free blood plasma after the last washing procedure. These suspensions contained native intact RBCs and plasma proteins, giving the possibility of forming aggregates at low shear rates and are called "RBC plasma."

The hematocrit was determined using a red blood cell counter (Micros 60 OT 18, ABX Diagnostics, Montpellier, France). All samples were oxygenated in excess of 98%. Lower oxygen saturations may lead to drastically different results in the optical parameters.[11] The oxygen saturation was determined with a blood gas analyzer (OPTI Care, AVL Medizintechnik GmbH, Bad Homburg). A miniaturized blood circulation setup was used with a roller pump (Sorin Group, Germany) and a blood reservoir, which was constantly aerated with a gas mixture of O_2, N_2, and CO_2. The temperature was kept constant at 20°C. The blood was gently stirred to avoid uncontrolled sedimentation or cell aggregation within the reservoir. The blood was kept flowing by a customized turbulence-free cuvette with laminar flow and a sample thickness of 116 μm. The flow was adjusted for each sample to keep constant wall shear rates of 0, 50, 100, 200, 600, and 1000 s^{-1} at the cuvette windows.

2.2 *Spectral Measurements*

The diffuse reflectance R_d, the total transmission T_t, and the diffuse transmission T_d of all blood samples were measured using an integrating sphere spectrometer (Perkin Elmer, Lambda 900, Rodgau-Jügesheim, Germany) in the spectral range of 250 to 1100 nm at data intervals of 5 nm. The experimental setup was described by Friebel et al.,[6] and allowed the measurement of macroscopic radiation distribution with an error of less than 0.1%. A special iMCS program was used which, taking into consideration various radiation losses, gives valid results for the calculated intrinsic optical parameters.[1] Hct-dependent effective phase functions for RBCs flowing with a shear rate of 600 s^{-1} was evaluated previously using the double integrating sphere technique.[6] For shear rate changes, no significant dependence on the phase function could be observed. This is due to the relatively small shear-rate dependent changes in the optical parameters com-

pared to Hct changes. Therefore, effective phase functions determined for 600 s^{-1} were used for all shear rates in the range 0 to 1000 s^{-1}. The iMCS was carried out using the Reynolds-McCormick phase[34] function with $\alpha=1.6$ for Hct 8.6% and $\alpha=1.7$ for Hct 42.1%. The error in this method for selecting phase functions can lead to deviations in the determination of the optical parameters of ±1% for μ_a, ±2% for μ_s, ±2% for $(1-g)$, and ±1.5% for μ_s'. An error threshold of 0.1%, i.e., the difference between measured and simulated macroscopic radiation distribution, was used for the simulation of the intrinsic optical parameters of blood. For all blood samples, a total of three independent measurement series were carried out and independently simulated using about 10^7 photons for each simulation. The standard deviation of the three measurements was 2 to 5% for μ_a, μ_s, $(1-g)$, and μ_s', as is shown in the diagrams.

3 Results

To exclude the optical influence of biological variability of RBC samples with identical Hct taken from different donors, all intrinsic optical parameters given in this work are relative values related to those determined at a standard shear rate of 600 s^{-1}. The absolute values can be obtained by multiplication with the averaged parameters of standard blood of the same Hct, which was measured under standard conditions (wall shear rate 600 s^{-1}, oxygen saturation 98 to 100%, osmolarity 300 mosmol/l, pH 7.4, 20°C) and was presented in a previous paper.[15]

To reduce the number of diagrams, only the optical parameters dependent on wavelength for RBCs in NaCl have been selected to be shown in Figs. 1–4. In Fig. 5, the wavelength dependency of μ_a and μ_s' for RBCs in plasma is exemplarily shown for diluted blood.

The fixed cells were investigated at the shear rates used for native RBCs in NaCl, but only the mean values of the relative optical properties at 1000 s^{-1} have been shown, because at lower shear rates, no significant difference could be found. RBCs in plasma are only measured and shown at flow stop and 600 s^{-1} to investigate the formation of aggregates.

The measurements on native RBCs in NaCl and in plasma were carried out using Hct 42.1% and 8.4%, but because of similar results, only the data from the investigations on Hct 42.1% were shown in Figs. 1–4. In Sec. 3.5 and Fig. 5, selected specific characteristics are presented from diluted blood.

3.1 *Absorption*

Figure 1(a) shows the relative values of μ_a of RBC suspended in saline solution with Hct 42.1% dependent on wavelength for six different wall shear rates. With regard to the error tolerance, the relative absorption coefficient μ_a_rel for all adjusted shear rates is constant throughout the investigated wavelength range, so that a mean relative absorption coefficient can be calculated for 250 nm$<\lambda<$1100 nm. The mean relative values of RBCs in saline solution (RBC in NaCl), of fixed RBCs (RBC fixed), and RBC suspended in plasma (RBC plasma), are presented in Fig. 1(b) dependent on shear rate.

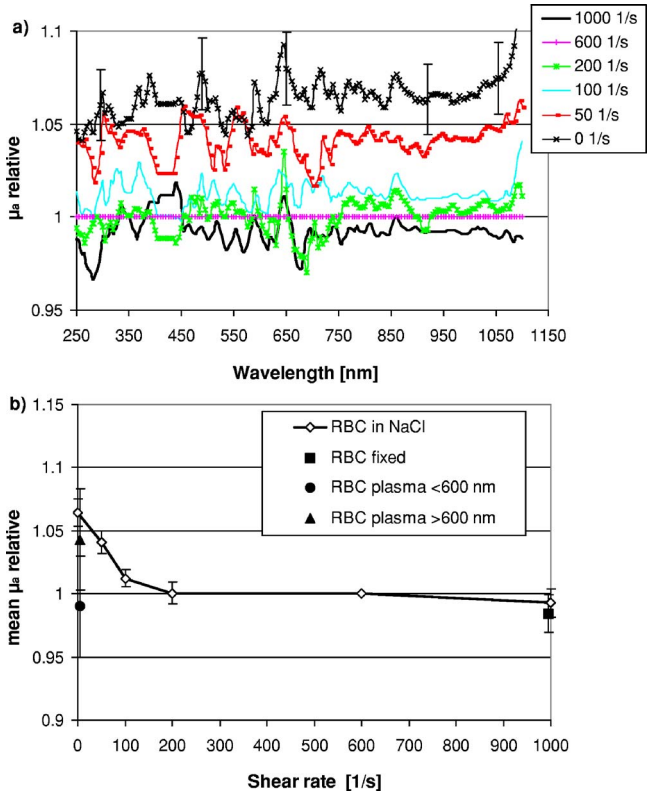

Fig. 1 (a) μ_a_rel of RBC in saline solution with Hct 42.1% dependent on wavelength for six different wall shear rates. (b) Mean values of μ_a_rel of the spectral range 250 to 1100 nm of native and fixed RBC in saline solution dependent on wall shear rate, and the mean values of μ_a_rel of RBC in plasma at flow stop for the wavelength ranges 250 to 600 nm and 600 to 1100 nm.

The mean relative absorption of RBCs in saline solution is at a maximum at 1.064±0.01 at flow stop. With increasing shear rates, the mean μ_a_rel decreases continuously to a value of 1.0±0.009 at 200 s^{-1}. Above 200 s^{-1}, μ_a_rel shows no significant change up to 1000 s^{-1} with a value of 0.993±0.015. The fixed RBCs in saline solution show a comparable shear rate value within the error tolerance. RBCs suspended in plasma show wavelength-dependent effects at flow stop. For the RBCs in plasma, the absorption in the wavelength range 250 to 600 nm is lower than in the range 600 to 1100 nm. For this reason, two mean values are presented for RBCs in plasma in Fig. 1(b), one mean value for μ_a_rel with $\lambda<600$ nm and one for μ_a_rel with $\lambda>600$ nm. Mean μ_a_rel values decreased to 0.99±0.04 in the wavelength range below 600 nm, whereas above 600 nm, μ_a_rel had a mean value of 1.043±0.04.

3.2 *Scattering*

Figure 2(a) shows the relative values of μ_s dependent on wavelength for different shear rates of RBCs in saline solution. As observed for the absorption, μ_s_rel of RBCs suspended in saline solution shows no significant dependence on wavelength but is significantly influenced by changes in the shear rate. The mean μ_s_rel is with 1.2±0.03 at a maximum at flow stop, and decreases substantially with increasing shear rate up to 1.05±0.02 at 100 s^{-1} [Fig. 2(b)]. Above 100 s^{-1},

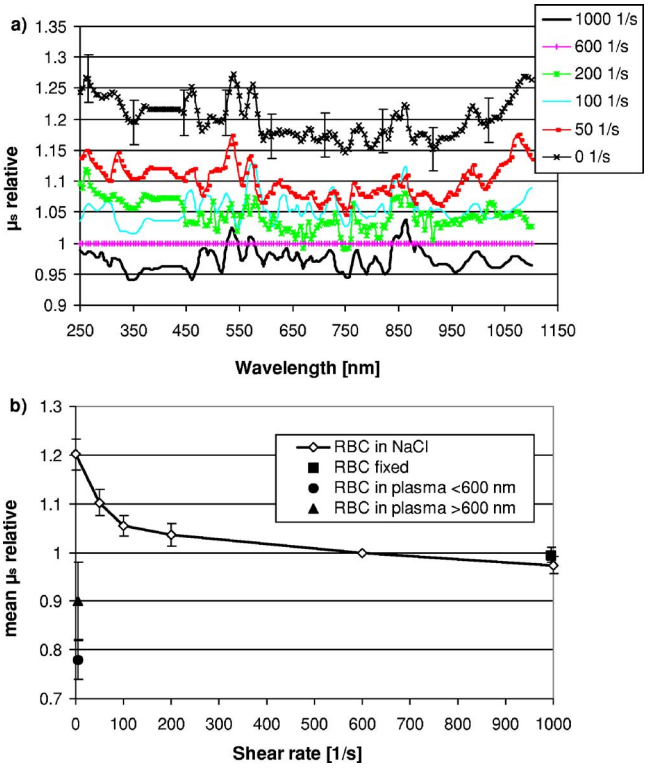

Fig. 2 (a) μ_s_rel of RBC in saline solution with Hct 42.1% dependent on wavelength for six different wall shear rates. (b) Mean values of μ_s_rel of the spectral range 250 to 1100 nm of native and fixed RBC in saline solution dependent on wall shear rate, and the mean values of μ_s_rel of RBC in plasma at flow stop for the wavelength ranges 250 to 600 nm and 600 to 1100 nm.

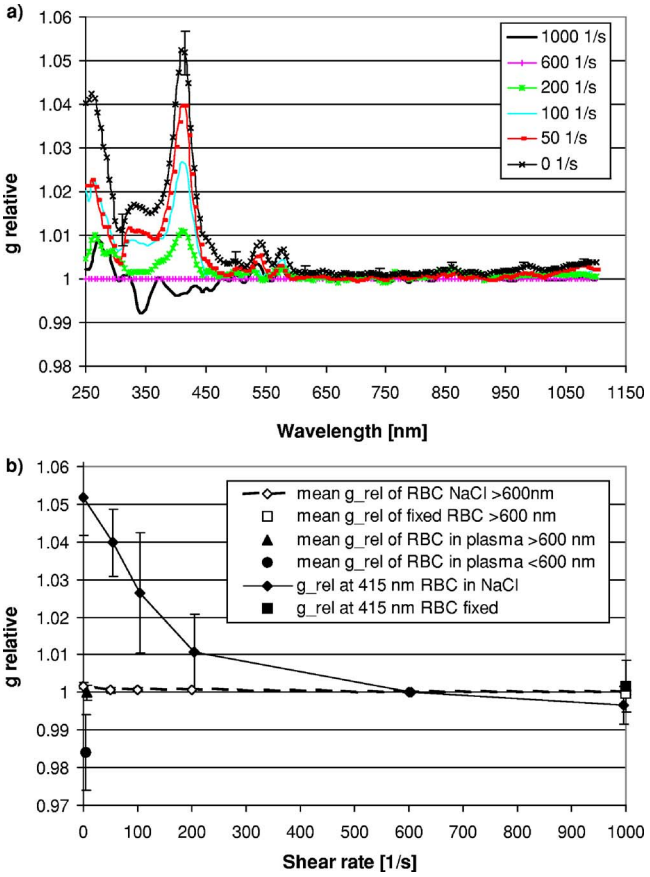

Fig. 3 (a) g_rel of RBC in saline solution with Hct 42.1% dependent on wavelength for six different wall shear rates. (b) Mean values of g_rel of 415 nm and the spectral range 600 to 1100 nm of native and fixed RBC in saline solution dependent on wall shear rate, and the mean values of g_rel of RBC in plasma at flow stop for the wavelength ranges 250 to 600 nm and 600 to 1100 nm.

μ_s_rel decreases slightly to a value of 1.037±0.02 at 200 s^{-1}, and finally to 0.974±0.016 at 1000 s^{-1} [Fig. 2(b)]. For fixed RBC, μ_s_rel is equivalent to the values of native RBC up to 600 s^{-1}. At 1000 s^{-1}, μ_s_rel is slightly higher with a value of 0.995.

Corresponding to μ_a_rel, also for μ_s_rel of RBCs suspended in plasma, two averaged values at flow stop for the wavelength ranges 250 to 600 nm (0.78±0.04) and above 600 nm (0.9±0.08) can be differentiated, which are considerably smaller than the values for RBCs in saline solution.

3.3 *Anisotropy*

Figure 3(a) shows the relative values of the anisotropy factor g of RBCs suspended in saline solution for different wall shear rates dependent on wavelength. In contrast to μ_a_rel and μ_s_rel, g_rel shows a wavelength dependence below 600 nm. Regarding the statistical uncertainty of the simulation, g_rel shows no significant changes above 600 nm with regard to shear rate and wavelength. Nevertheless, a mean g_rel averaged over this spectral range was calculated for each shear rate and is depicted versus the shear rate in Fig. 3(b), including g_rel at 415 nm, to characterize the shear rate dependence in the highly absorbing spectral range. Analogous values were determined for fixed RBCs at 1000 s^{-1}. Two average values for the wavelength ranges were calculated above and below 600 nm for RBCs suspended in plasma at flow stop.

In the wavelength range 600 to 1100 nm, g_rel of RBCs in saline solution is only at 1.002±0.0008, significantly higher than at 600 s^{-1} at flow stop. At 1000 s^{-1}, g_rel of the fixed RBC is not affected, resulting in values of about 1.

By contrast, at 415 nm, g_rel of untreated RBCs in saline solution has a value of 1.052±0.01 at a maximum at flow stop. With increasing shear rates, g_rel decreases asymptotically to values of 1.01±0.01 at 200 s^{-1} and 0.997±0.005 at 1000 s^{-1}.

The g_rel values of fixed RBCs at 415 nm at a shear rate of 1000 s^{-1} show a slight increase to 1.002±0.005, and for the spectral range above 600 nm, the g_rel is comparable to the native RBCs in saline solution. At flow stop, g_rel of RBCs suspended in plasma remains at 1 in the wavelength range above 600 nm. However, in the range 250 to 600 nm, the mean g_rel decreases to 0.984±0.01.

3.4 *Effective Scattering Coefficient*

Figure 4(a) gives the calculated relative values of the effective scattering coefficient μ_s'_rel versus wavelength for different shear rates. Corresponding to the anisotropy factor, μ_s'_rel shows a different behavior below and above 600 nm. In the range above 600 nm, the mean μ_s'_rel of RBCs in saline

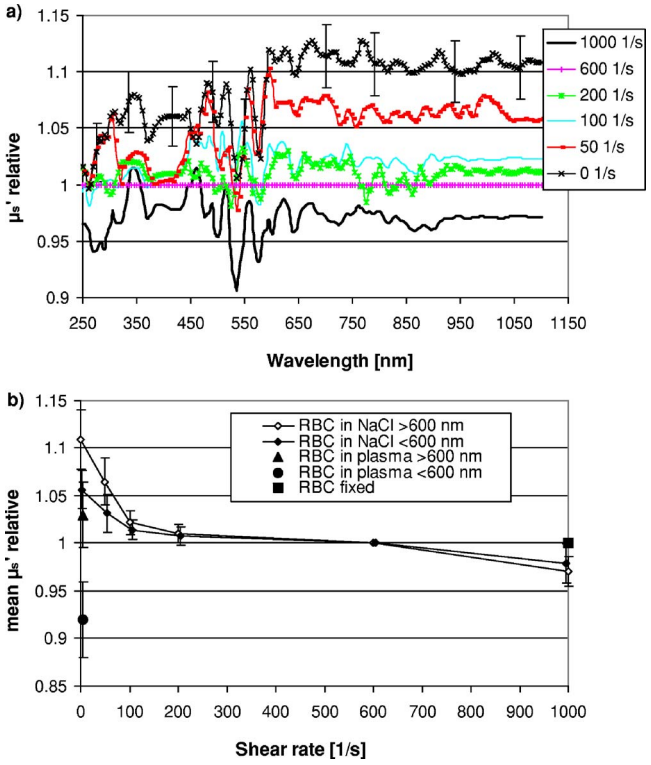

Fig. 4 (a) μ_s'_rel of RBC in saline solution with Hct 42.1% dependent on wavelength for six different wall shear rates. (b) Mean values of μ_s'_rel of native RBC in saline solution dependent on wall shear rate and the mean values of μ_s'_rel of RBC in plasma at flow stop for the wavelength ranges 250 to 600 nm and 600 to 1100 nm.

solution is at a maximum with 1.11±0.03 [Fig. 4(b)] at flow stop, and decreases significantly with increasing shear rate to 1.02±0.01 at 100 s^{-1}. Above 100 s^{-1}, there is a slight decrease in μ_s'_rel to 1.01±0.01 at 200 s^{-1}, and finally to 0.97±0.015 at 1000 s^{-1}. In the wavelength range 250 to 600 nm, μ_s'_rel shows with 1.056±0.02 at flow stop, and 1.03±0.02 at 50 s^{-1}, significantly lower μ_s'_rel values than above 600 nm. At a shear rate of 1000 s^{-1}, μ_s'_rel is, in the range 250 to 600 nm, with a value of 0.97±0.015, not significantly higher than above 600 nm. The fixed RBCs show slightly higher μ_s'_rel values of 1 at 1000 s^{-1} for both spectral ranges.

For RBCs suspended in plasma at flow stop, μ_s'_rel results in a mean value of 0.92±0.04 in the wavelength range 250 to 600 nm and 1.03±0.03 in the range 600 to 1100 nm.

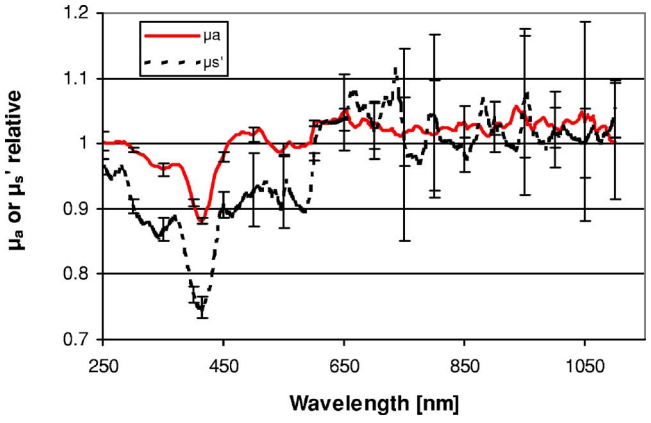

Fig. 5 μ_a_rel and μ_s'_rel of RBC suspended in plasma with a Hct of 8.6% at flow stop compared to a shear rate of 600 s^{-1} in the wavelength range 250 to 1100 nm.

3.5 *Diluted Blood*

With regard to statistical uncertainties, the experiments on blood (Hct of 8.6%) lead to comparable results for the relative values, which indicate that there is no significant Hct dependence of shear-rate induced changes on the optical properties of blood in this Hct range. However, the determination of the optical parameters below 600 nm, where the absorption of hemoglobin is high, showed reduced statistical errors due to the low optical density of *diluted* blood. The shear-rate induced changes in particular in the optical parameters of RBCs suspended in plasma could be analyzed more precisely. Figure 5 shows the spectrum from 250 to 1100 nm of the relative values of μ_a and μ_s' of RBCs suspended in plasma with an Hct of 8.6% at flow stop, compared to a shear rate of 600 s^{-1}. The spectrum of μ_a_rel is the mirror image of the absorption spectrum of hemoglobin. The mean values of μ_a_rel, averaged over the wavelength ranges 250 to 600 nm (0.98±0.03), and 600 to 1100 nm (1.027±0.03), are comparable to those of Hct 42.1% [see Fig. 1(b)]. In the same way, the spectrum of μ_s'_rel represents the inverse absorption spectrum. The mean values for the wavelength range 250 to 600 nm are 0.89±0.05 and 1.02±0.03 for the range 600 to 1100 nm, and also correspond to those of Hct 42.1% [see Fig. 4(b)]. Analogous results were obtained for the parameters μ_s_rel and g_rel. This indicates that the wavelength dependence of the decrease in absorption and scattering of aggregated RBC is correlated with the hemoglobin absorption. This phenomenon should be also assumed for physiological Hct levels such as 42.1%.

4 Discussion

4.1 *Red Blood Cell Aggregation at Flow Stop*

Cell aggregation of RBCs suspended in plasma at flow stop compared to RBCs in saline solution leads to a decrease in optical parameters that is correlated with the absorption of hemoglobin. The decrease of μ_a and the enhanced effect at high absorption can be explained by the sieve effect. Photons that do not hit red blood cells pass unattenuated by absorption. This leads to a reduced absorption effect comparable to homogeneously dispersed hemoglobin. Aggregation of RBCs leads to a more heterogeneous dispersion of the absorbing hemoglobin and therefore to greater absorption reduction. The sieve effect increases considerably with absorption[6,35] and aggregation. This phenomenon, also called absorption flattening, is in agreement with the results of the measurements at Hct 8.6% presented in Fig. 5, which shows the correlation between the absorption and the decrease of μ_a_rel at flow stop. The same result can be obtained by Mie calculations assuming spherical aggregates of 2, 3, and 4 times the single RBC volume. In this case, the increase in the absorption cross section is lower than the evoked decrease in concentration of the

growing aggregates, leading to a decrease of its product, the absorption coefficient. This phenomenon increases with the size of the aggregates and with hemoglobin absorption. An aggregate of three-fold volume, for example, leads to a reduction in μ_a to 99% in the wavelength range 600 to 1100 nm and to 77% at 415 nm.

The decrease of μ_s_rel, g_rel, and μ_s'_rel due to RBC aggregation is analogous to the saturation effect of the linear increase of μ_s and μ_s' with Hct and the Hct-dependent decrease of g, demonstrated by Meinke et al.[15] Induced by the high cell concentration with very small cell-to-cell distances, aggregated or loosely associated double or triple cells occur under flow conditions. This effect leads to collective scattering with a decrease in the scattering cross section per cell, and consequently to an attenuation of the linear increase of μ_s and μ_s', with Hct. Furthermore, the collective scattering induces a reduction of the forward scattering, thus reducing g. These effects were shown to increase with absorption, i.e., with the imaginary part of the complex refractive index. As a consequence, cell aggregation at constant Hct leads to an absolute decrease of μ_s, μ_s', and g, which is enhanced by μ_a.

The results of μ_s and g in the wavelength range 600 to 1100 nm are in qualitative agreement with the results of T-matrix computations of spheroids by Eneijder et al.[20] This work shows cell-aggregation induced reduction of the scattering cross section and relative changes in g of about 0.003, which are below the measurement errors of the respective values presented here. Furthermore, results of μ_a and μ_s' in the wavelength range 600 to 1100 nm correspond to the absorption- and effective scattering coefficients of undiluted bovine blood at flow stop. These were experimentally determined by Eneijder et al., who found μ_a and μ_s' to be approximately 1.03, relative to a shear rate of 800 s^{-1} at 800 nm. In this investigation, the parameters were found to be independent of wavelength in the range 650 to 900 nm, where the absorption is low.

The aggregation induced decrease of μ_a and μ_s are consistent with the findings of Shvartsman and Fine,[16] who suggested that the natural pulsatile signal is driven by shear-force originated fluctuations of aggregation length.

4.2 *Shear Rate Range 0 to* 200 s^{-1}

Untreated RBCs suspended in saline solution are randomly oriented at flow stop and have a maximum absorption and scattering coefficient, and therefore a maximum absorption and scattering cross section per cell, because cell concentration does not change. Cell morphology associated with higher degrees of organization, such as aligned RBCs, exhibited lower scattering coefficients as explained by T-matrix computations.[20] At increasing shear rates, a decrease in the random cell orientation reduces this effect, and as a consequence, the cross sections of μ_a and μ_s decrease asymptotically. Above a shear rate of 200 s^{-1}, only minimal changes can be observed, indicating that most of the effect has vanished. The same effect shows μ_s' and g in the wavelength range below 600 nm.

The Fahraeus effect, i.e., the dynamic decrease of the Hct, should also cause a decrease in the cell concentration dependent parameters μ_a_rel and μ_s_rel with increasing shear rate. At flow stop, the hematocrit is identical with the static hematocrit determined during blood preparation. Under flow conditions, a reduced dynamic Hct appears, which decreases with increasing shear rates. According to Barbee and Cokelet,[31] the relative Hct decrease can be estimated to be 9.5% for a vessel diameter of 116 μm. In flow cuvettes with a flat cross section, this effect should be smaller than in tubes, due to the mainly 2-D parabolic flowing profile, but it could also be responsible for a significant part of the measured relative μ_a and μ_s changes of 6.4 and 17%. Since the anisotropy factor g is not directly dependent on cell concentration, g_rel should not be influenced by the Fahraeus effect.

The anisotropy factor is proportional to the degree of absorption. At 415 nm where the absorption is at a maximum, g_rel has the highest value for randomly oriented cells. In spectral regions where μ_a is very low (<0.1 mm^{-1}), g is almost invariant to changes in shear rate. The principle shape of the anisotropy spectra has been discussed in Friebel et al.[6] The spectrum of the absolute anisotropy factor at a wall shear rate of 600 s^{-1} is inversely related to the hemoglobin absorption, i.e., 415 nm is at a minimum. The absorption-dependent decrease in g of undiluted RBC suspensions shows the highest deviation to the predictions of the Mie theory[36] compared with other optical parameters. The Mie theory shows a similar influence of the absorption on g, but only at absorption values that are 10 times higher than those of blood. The fact that reducing cell alignment and deformation will cause g to increase, a disproportionally high value in the spectral regions of high absorption indicates an approximation to the Mie theory. The same effect could be observed in ongoing investigations when the RBCs were made to swell to more spheroid forms by reducing the osmolarity.

μ_s' also shows a maximum at flow stop, but the maximum decreases with increasing absorption, which is the expected inverse behavior of the anisotropy factor. The values of μ_s' in the wavelength range 600 to 1100 nm are in accordance with the measurements on whole bovine blood at 800 nm of Eneijder et al.,[20] who found μ_s'_rel with over 1.05 at a shear rate of 100 s^{-1}.

Roggan et al.[1] found relative μ_a and μ_s' values of 1.09 and 1.11 at flow stop for RBCs in saline solution of Hct 41% at 633 nm, which are comparable to the values presented in these investigations.

4.3 *Shear Rate Range 200 to* 600 s^{-1}

In this shear rate range, the red blood cells start to align with the flow, and the aggregates of RBCs in plasma are completely dissociated.[37] The absorption cross section does not change within this shear rate range, indicating that cell alignment has no significant influence on μ_a, and the dynamic Hct decrease is only effective in the shear rate range from 0 to 200 s^{-1}. As the Fahraeus effect has the same influence on μ_a and μ_s, it can be concluded that the small additional decreasing effect on μ_s_rel of 3.7% is only evoked by a decrease in the cross section induced by increasing cell alignment and decreasing random cell orientation. The latter also causes the slight decrease in the relative anisotropy factor, in the spectral range below 600 nm, because g is not directly dependent on cell concentration. As a consequence, a decrease of μ_s'_rel of about 1% is also induced by cell alignment and decreasing

random cell orientation. There is partial agreement with the results of Steenbergen, Kolkman, and de Mul,[38] who found that by using inverse MCS, the total attenuation coefficient $\mu_t = \mu_a + \mu_s$ of undiluted blood in plasma measured by within a 100-μm cuvette at 633 nm, is approximately constant in the shear rate range 150 to 500 s^{-1}. However, below 150 s^{-1}, there is a strong variation of μ_t possibly induced by clustering effects. In contrast, g was found to increase by 10% with the shear rate in the range 50 to 500 s^{-1} based on the assumption that the Henyey-Greenstein phase function[39] renders a satisfactory description for single scattering by whole blood, which is in contrast to the results of prior studies[6] and consequently to the method used in the present work.

4.4 *Shear Rates at* 1000 s^{-1}

At these high shear rates, RBCs start to elongate. The decrease in μ_s_rel when the shear rate is increased from 600 to 1000 s^{-1} does not occur when the cells are fixed, indicating that cell elongation has an additional decreasing effect on the scattering cross section. Cell elongation also reduces g_rel; the effect vanishes after cell fixation, which suggests that elongation causes a further higher degree of organization. At a shear rate of 1000 s^{-1}, the absorption coefficient of untreated and fixed cells shows no significant change compared to 600 s^{-1}, indicating that cell elongation as well as alignment has no influence on the absorption cross section.

The μ_a_rel and μ_s'_rel values of RBCs in saline solution, dependent on shear rate in the wavelength range 600 to 1100 nm, are in agreement with previous measurements of RBCs in saline solution of Hct 41% at 633 nm made by Roggan et al.,[1] who determined relative μ_a and μ_s' values of 0.96 and 0.97 (values interpolated) at a shear rate of 1000 s^{-1}. Furthermore, the T-matrix computations[20] of aligned and elongated spheroids in this spectral range resulted in a reduction of the scattering cross section and an almost unchanged g factor.

5 Conclusion

In the work presented here, it could be shown that the wall shear rate has an influence on the optical parameters μ_a, μ_s, g, and μ_s' of human blood induced by effects on the cell shape and cell organization of the RBCs. Moreover, a dependence was found to exist between the shear rate dependent effects and the hemoglobin absorption within the RBCs. The maximal absorption and scattering cross sections were found for randomly oriented RBCs. Increasing the shear rate leads to an asymptotic decrease in the absorption and scattering cross sections and of g at spectral ranges with high hemoglobin absorption. Up to a shear rate of 200 s^{-1}, a dynamic hematocrit decrease (Fahraeus effect) leads to reduction in the cell concentration and therefore to a further decrease in μ_a and μ_s. At low absorption, g is almost independent of shear rate. μ_s' values decrease with the shear rate, but this behavior is attenuated to increasing hemoglobin absorption. Cell aggregation at flow stop leads to an absorption-dependent decrease in μ_a, μ_s, g, and μ_s'. The decrease in μ_a can be explained by the sieve effect and by calculations for accreted spheres according to the Mie theory. An increase in collective scattering leads to a reduction of the scattering cross section per cell and the forward scattering. Measurements on diluted blood with Hct 8.6% showed no significant differences in the shear rate dependence of the optical parameters.

From these results, it follows that to estimate the optical properties of blood, the flow conditions have to be taken into account. Moreover, not only the collective scattering phenomena but also the absorption within the cell, together with the cell shape, are important parameters for the scattering properties of blood.

Acknowledgments

This work was supported by the Federal Ministry of Education and Research (grant number 13N7522). The authors also wish to thank the Sorin Group Deutschland GmbH, Munich, for placing the equipment at our disposal. The blood bags were kindly provided by the Departments of Transfusion Medicine, Charité-Universitätsmedizin Berlin, Germany.

References

1. A. Roggan, M. Friebel, K. Dörschel, A. Hahn, and G. Müller, "Optical properties of circulating human blood in the wavelength range 400–2500 nm," *J. Biomed. Opt.* **4**(1), 36–46 (1999).
2. M. Friebel and M. Meinke, "Determination of the complex refractive index of highly concentrated hemoglobin solutions using transmittance and reflectance measurements," *J. Biomed. Opt.* **10**, 064019 (2005).
3. L. G. Lindberg and P. A. Öberg, "Optical properties of blood in motion," *Opt. Express* **32**(2), 253–257 (1993).
4. M. Meinke, G. Müller, J. Helfmann, and M. Friebel, "Optical properties of platelets and blood plasma and their influence on the optical behaviour of whole blood in the VIS-NIR wavelength range," *J. Biomed. Opt.* **12**, 014024 (2007).
5. A. N. Yaroslavsky, I. V. Yaroslavsky, T. Goldbach, and H. J. Schwarzmaier, "The optical properties of blood in the near infrared spectral range," *Proc. SPIE* **2678**, 314–324 (1996).
6. M. Friebel, A. Roggan, G. Müller, and M. Meinke, "Determination of optical properties of human blood in the spectral range 250–1100 nm using Monte Carlo simulations with hematocrit-dependent effective scattering phase functions," *J. Biomed. Opt.* **11**(3), 031021 (2006).
7. M. Hammer, D. Schweitzer, B. Michel, E. Thamm, and A. Kolb, "Single scattering by red blood cells," *Appl. Opt.* **37**(31), 7410–7418 (1998).
8. A. Nilsson, P. Alsholm, A. Karlson, and S. Andersson-Engels, "T-matrix computation of light scattering by red blood cells," *Appl. Opt.* **37**(13), 2735–2748 (1998).
9. J. M. Steinke and A. P. Sheperd, "Comparision of Mie theory and light scattering of red blood cells," *Appl. Opt.* **27**(19), 4027–4033 (1988).
10. D. J. Faber, F. J. van der Meer, M. C. G. Aalders, D. M. de Bruin, and T. G. van Leeuwen, "Hematocrit-dependence of the scattering coefficient of blood determined by optical coherence tomography," *Proc. SPIE* **5861**, 58610W (2005).
11. D. J. Faber, M. C. G. Aalders, E. G. Mik, B. A. Hooper, M. J. C. van Gemert, and T. G. van Leeuwen, "Oxygen saturation-dependent absorption and scattering of blood," *Phys. Rev. Lett.* **93**, 028102 (2004).
12. M. Meinke, I. Gersonde, M. Friebel, J. Helfmann, and G. Müller, "Chemometric determination of blood parameters using visible near-infrared spectra," *Appl. Spectrosc.* **59**(6), 826–835 (2005).
13. J. Lademann, H. Richter, W. Sterry, and A. V. Priezzhev, "Diagnostic potential of erythrocytes aggregation and sedimentation measurements in whole blood," *Proc. SPIE* **4263**, 106–111 (2003).
14. A. Priezzhev, O. M. Ryaboshapka, N. N. Firsov, and I. V. Sirko, "Aggregation and disaggregation of erythrocytes in whole blood: Study by backscattering technique," *J. Biomed. Opt.* **4**(1), 76–84 (1999).
15. M. Meinke, G. Müller, J. Helfmann, and M. Friebel, "Empirical model functions to calculate the optical properties of human blood in the spectral range 250–1100 nm dependent on Hematocrit," *Appl. Opt.* **46**, 1742–1753 (2007).
16. L. D. Shvartsman and I. Fine, "Optical transmission of blood: Effect

of erythrocyte aggregation," *IEEE Trans. Biomed. Eng.* **50**, 1026–1033 (2003).
17. V. S. Lee and L. Tarassenko, "Absorption and multiple scattering by suspensions of aligned red blood cells," *J. Opt. Soc. Am. A* **8**(7), 1135–1141 (1991).
18. R. Bayer, S. Çaglayan, and B. Günther, "Discrimination between orientation and elongation of RBC in laminar flow by means of laser diffraction," *Proc. SPIE* **2136**, 105–113 (1994).
19. A. H. Gandjbakhche, P. Mills, and P. Snabre, "Light-scattering technique for the study of orientation and deformation of red blood cells in a concentrated suspension," *Appl. Opt.* **33**(6), 1070–1078 (1994).
20. A. M. K. Enejder, J. Swartling, P. Aruna, and S. Andersson-Engels, "Influence of cell shape and aggregate formation on the optical properties of flowing whole blood," *Appl. Opt.* **42**(7), 1384–1394 (2003).
21. H. J. Klose, E. Volger, H. Brechtelsbauer, and H. Schmid-Schönbein, "Microrheology and light transmission of blood," *Pfluegers Arch.* **333**, 126–139 (1972).
22. K. Sakamoto and H. Kanai, "Electrical characteristics of flowing blood," *IEEE Trans. Biomed. Eng.* **BME-26**, 686–695 (1979).
23. H. Schmid-Schönbein and R. Wells, "Fluid drop-like transition of erythrocytes under shear," *Science* **165**, 288–291 (1969).
24. H. Schmid-Schönbein, K. A. Kline, L. Heinrich, E. Volger, and T. Fischer, "Microrheology and light transmission of blood. III. The velocity of red cell aggregate formation," *Pfluegers Arch.* **354**, 299–317 (1975).
25. S. Chien, "Biophysical behaviour of red cells in suspensions," in *The Red blood Cell*, 2nd ed., Vol. **2**, D. M. Surgenor, Ed., pp. 1031–1133, Academic Press, New York (1975).
26. A. Hahn, A. Roggan, and D. Schädel, "Die optischen Eigenschaften von dicken Schichten zirkulierendem Humanblutes," *D. Minimal Invas. Med.* **7**, 79–90 (1996).
27. A. V. Priezzhev, N. B. Savchenko, and B. A. Levenko, "Laser Doppler monitoring of alterations in fish embryo flow in response to external stimuli," *Proc. SPIE* **2678**, 409–415 (1996).
28. M. Donner and J. F. Stolz, "Erythrocytes aggregation approach by light scattering determination," *Biorheology* **25**, 367–375 (1988).
29. N. N. Firsov, A. V. Priezzhev, O. M. Ryaboshapka, and I. V. Sirko, "Aggregation and disaggregation of erythrocytes in whole blood: study by backscattering technique," *J. Biomed. Opt.* **4**, 76–84 (1999).
30. J. Lademann, H. J. Weigmann, W. Sterry, A. Roggan, G. Müller, A. V. Priezzhev, and N. N. Firsov, "Investigation of the aggregation and disaggregation properties of erythrocytes by light scattering measurements," *Laser Phys.* **9**(1), 357–62 (1999).
31. J. H. Barbee and G. R. Cokelet, "The Fahraeus effect," *Microvasc. Res.* **3**, 6–16 (1971).
32. P. Gaehtgens, K. H. Albrecht, and K. Kreutz, "Fahraeus-effect and cell screening during tube flow of human blood. I. Effect of variation of flow rate," *Biorheology* **15**, 147–154 (1978).
33. I. M. Krieger, "Shear rates in the Couette viscometer," *Trans. Soc. Rheol.* **12**, 5–11 (1968).
34. L. Reynolds and N. McCormick, "Approximate two-parameter phase function for light scattering," *J. Opt. Soc. Am.* **70**, 1206–1212 (1980).
35. R. N. Pittman, "In vivo photometric analysis of hemoglobin," *Ann. Biomed. Eng.* **14**, 119–137 (1986).
36. G. Mie, "Pioneering mathematical description of scattering by spheres," *Ann. Phys.* **25**, 337 (1908).
37. H. Schmid-Schönbein, E. Volger, and H. J. Klose, "Microrheology and light transmission of blood II. The photometric quantification of red cell aggregate formation and dispersion in flow," *Pfluegers Arch.* **333**, 140–155 (1972).
38. W. Steenbergen, R. Kolkman, and F. de Mul, "Light scattering properties of undiluted human blood subjected to simple shear," *J. Opt. Soc. Am. A* **16**, 2959–2967 (1999).
39. L. G. Henyey and J. L. Greenstein, "Diffuse radiation in the galaxy," *Astrophys. J.* **93**, 70–83 (1941).